AIAA 81-1008R

Generalized Coordinate Forms of Governing Fluid Equations and Associated Geometrically Induced Errors

Richard G. Hindman*
Iowa State University, Ames, Iowa

The governing equations of fluid flow may be cast into various forms upon application of a generalized coordinate mapping. These forms are the nonconservation law form (NCLF) and strong, weak, and chain rule conservation law forms (SCLF, WCLF, CRCLF, respectively). This paper describes the geometrically induced errors resulting from the failure to satisfy a certain consistency condition for each of these four forms and also demonstrates the ability of the CRCLF to produce exactly the same numerical solution as the WCLF, provided a condition is met on where to evaluate the transformation metrics. It is also demonstrated that considerably fewer arithmetic operations are required to advance the solution from n to $n+1$ when the CRCLF is used in comparison to both the SCLF and WCLF.

Introduction

THE effort devoted to the field of computational fluid dynamics is progressing at an ever-increasing rate. At certain points in time during this natural evolution of numerical methods, schemes, and ideas it is sometimes instructive to pause to reflect upon past work in an attempt to gain the proper perspective. It is important that this reflection reaches all of the way to the fundamental rules and practices used to develop numerical techniques. Some of these practices are often taken for granted much too soon after their introduction into the literature. Only through a global view of this past effort can subtle, mutually experienced problem areas and possible causes be identified.

The present work deals with the numerical solution to the transformed fluid flow equations (i.e., Euler equations, etc.) using the finite-difference approach. The transformed equations are obtained through application of a generalized mapping from physical coordinates to computational coordinates. At the time of application of the mapping to the original equations and prior to choosing the numerical integration scheme, the analyst must decide in which form the equations should be written. The choices are the nonconservation law form (NCLF), strong conservation law form (SCLF), weak conservation law form (WCLF), and chain rule conservation law form (CRCLF). This decision is one of the fundamental practices alluded to in the previous paragraph. The present work illustrates how such a fundamental decision can strongly influence both the amount of analysis required to develop a consistent algorithm and the number of arithmetic operations required to execute the algorithm. In addition, it is shown that large solution errors and in some cases instabilities can result from failure to implement the results of such an analysis.

Governing Equations

The present work applies to problems governed by equations having the following form

$$\frac{\partial u}{\partial t}+\nabla\cdot\tilde{f}=0 \tag{1}$$

where ∇ is the gradient operator, u the dependent variable vector, and $\tilde{f}$ (in general) the dyadic flux function of the vector u and its gradient. Both the Euler and Navier-Stokes equations governing fluid flow problems can be expressed in this form. The present work concentrates on equations with not more than two space dimensions, although extension of the analysis and results to three space dimensions is straightforward.

Since most engineering problems are seldom solvable in a Cartesian coordinate system, a generalized coordinate mapping is often introduced in the form (for flows with two space dimensions and time)

$$\tau=t,\quad \xi=\xi(t,x,y),\quad \eta=\eta(t,x,y) \tag{2}$$

The gradient operator ∇ in terms of these new coordinates is given by

$$\nabla=\nabla\xi\frac{\partial}{\partial\xi}+\nabla\eta\frac{\partial}{\partial\eta}$$

and the operator $\partial/\partial t$ transforms to

$$\frac{\partial}{\partial\tau}+\xi_t\frac{\partial}{\partial\xi}+\eta_t\frac{\partial}{\partial\eta}$$

The dyadic $\tilde{f}$ is defined as $\tilde{f}=\hat{i}f+\hat{j}g$ where f and g are flux vectors associated with the x or $\hat{i}$ direction and y or $\hat{j}$ direction, respectively. The application of Eq. (2) to Eq. (1) yields

$$\frac{\partial u}{\partial\tau}+\xi_t\frac{\partial u}{\partial\xi}+\eta_t\frac{\partial u}{\partial\eta}+\xi_x\frac{\partial f}{\partial\xi}+\eta_x\frac{\partial f}{\partial\eta}+\xi_y\frac{\partial g}{\partial\xi}+\eta_y\frac{\partial g}{\partial\eta}=0 \tag{3}$$

This form of the transformed equations will be called the chain rule conservation law form (CRCLF). This equation may be written with the metric coefficients inside the differentiation, thus producing a source term. The resulting form is called the weak conservation law form (WCLF) and is given by

$$\frac{\partial u}{\partial\tau}+\frac{\partial(\xi_t u+\xi_x f+\xi_y g)}{\partial\xi}+\frac{\partial(\eta_t u+\eta_x f+\eta_y g)}{\partial\eta}+h=0 \tag{4}$$

Presented as Paper 81-1008 at the AIAA 5th Computational Fluid Dynamics Conference, Palo Alto, Calif., June 22-23, 1981; submitted June 24, 1981; revision received Feb. 22, 1982.

*Assistant Professor, Aerospace Engineering and Computational Fluid Dynamics Institute. Member AIAA.

where

$$h=-[(\xi_t)_\xi+(\eta_t)_\eta]u-[(\xi_x)_\xi+(\eta_x)_\eta]f$$
$$-[(\xi_y)_\xi+(\eta_y)_\eta]g$$

It has been shown by Viviand[1] that it is possible to write the transformed equations in strong conservation law form (SCLF) as

$$\frac{\partial}{\partial\tau}\left(\frac{u}{J}\right)+\frac{\partial}{\partial\xi}\left(\frac{\xi_t u+\xi_x f+\xi_y g}{J}\right)+\frac{\partial}{\partial\eta}\left(\frac{\eta_t u+\eta_x f+\eta_y g}{J}\right)=0 \tag{5}$$

where J is the transformation Jacobian given by

$$J=\xi_x\eta_y-\xi_y\eta_x$$

Thus far, all forms of the transformed equations have been referred to as conservation law forms. For the sake of completeness another form applicable to the Euler equations is included here. This is the nonconservation law form (NCLF) which may be obtained from Eq. (3) by recognizing that $f=f(u)$ and $g=g(u)$ so that

$$\frac{\partial f}{\partial\xi}=\frac{df}{du}\frac{\partial u}{\partial\xi},\quad \frac{\partial g}{\partial\xi}=\frac{dg}{du}\frac{\partial u}{\partial\xi},\quad \text{etc.}$$

In these expressions df/du and dg/du are Jacobian matrices to be denoted by A and B, respectively. Equation (3) is thus rewritten in NCLF as

$$\frac{\partial u^*}{\partial\tau}+(\xi_t I+\xi_x A+\xi_y B)\frac{\partial u^*}{\partial\xi}+(\eta_t I+\eta_x A+\eta_y B)\frac{\partial u^*}{\partial\eta}=0 \tag{6}$$

The superscript * on the dependent variable vector u indicates that in the NCLF the dependent variables are often chosen to be the so-called primitive variables rather than the conservative variables. This choice affects the appearance of the Jacobian matrices A and B but not their characteristic structure.

For later reference, it will be noted that the transformation metrics in Eqs. (3-6) are related to the metrics of the inverse mapping through the identities

$$\frac{\xi_t}{J}=y_\tau x_\eta-x_\tau y_\eta \qquad \frac{\eta_t}{J}=x_\tau y_\xi-y_\tau x_\xi$$

$$\frac{\xi_x}{J}=y_\eta,\quad \frac{\xi_y}{J}=-x_\eta,\quad \frac{\eta_x}{J}=-y_\xi,\quad \frac{\eta_y}{J}=x_\xi \tag{7}$$

Equations (3-6) represent four distinct forms in which the transformed flow equations may be written. In developing a numerical algorithm to solve these equations, the analyst must decide which form best suits the purpose of the algorithm. Once this decision is made, a test is needed to determine the relative merit of the resulting algorithm. The remainder of this paper is devoted to one such test and its implications on the various forms of the transformed equations.

Uniform Flow Reproduction

One very simple test of a numerical integration algorithm is to initialize the entire computational mesh with a uniform rectilinear flow such that $u^n_{i,j}=\text{const}$ for all i,j in the mesh. The indices i,j correspond to the ξ and η directions, respectively, and the superscript n is the temporal index. Then advance the solution one step with the boundary values held fixed to obtain $u^{n+1}_{i,j}$ through the application of the numerical integration algorithm. If the algorithm is consistently formulated, the result must be $u^{n+1}_{i,j}\equiv u^n_{i,j}$ for all grid points. This test has been used by others[2-7] during algorithm development and checkout. Although the test is simple, it has far-reaching effects with regard to treatment of the transformation metric terms when either the SCLF or WCLF of the equations is used. The exact nature of these effects depends upon the particular numerical integration scheme chosen to integrate the governing equations. The test is automatically satisfied when either the NCLF or CRCLF of the equations is used. It should be noted that satisfaction of this test is by no means a sufficient condition for an algorithm to operate effectively nor is it strictly a necessary one. However, *it may be necessary* and the degree of necessary is a function of the geometric transformation. This fact is illustrated by the following example.

Application of MacCormack's[8] explicit predictor-corrector scheme to the transformed one-dimensional wave equation in WCLF

$$\frac{\partial u}{\partial t}+c\frac{\partial u}{\partial x}=0 \quad \overset{\tau=t}{\underset{\xi=\xi(x)}{\longrightarrow}} \quad \frac{\partial u}{\partial\tau}+\frac{\partial(c\xi_x u)}{\partial\xi}-c(\xi_x)_\xi u=0 \tag{8}$$

with the initial condition $u(\xi)=\text{const}$ at $t=0$ yields

Predictor

$$\overline{u^{n+1}}=u-\frac{\Delta\tau}{\Delta\xi}\Delta(c\xi_x u)+c\Delta\tau(\xi_x)_\xi u$$

Corrector

$$u^{n+1}=\frac{1}{2}\left[u+\overline{u^{n+1}}-\frac{\Delta\tau}{\Delta\xi}\nabla(c\xi_x u)^{\overline{n+1}}+c\Delta\tau(\xi_x)^{\overline{n+1}}_{\xi}\overline{u^{n+1}}\right]$$

where Δ and ∇ are the conventional forward and backward difference operators, respectively, and no subscript implies point j while no superscript implies temporal level n. Substitution of the predictor into the corrector and enforcement of $u^n_j=\text{const}$ for all j yields

$$u^{n+1}=u-\tfrac{1}{2}[(1+c\Delta\tau\bar{Q}-\nu\nabla\xi_x)(\nu\Delta\xi_x-c\Delta\tau Q)$$
$$+(\nu\nabla\xi_x-c\Delta\tau\bar{Q})-\nu\xi_{x_{j-1}}(\nu\nabla\Delta\xi_x-c\Delta\tau\nabla Q)]u$$

where $\nu\equiv c\Delta\tau/\Delta\xi$ and Q, $\bar{Q}$ are used to represent $(\xi_x)^n_\xi$ and $(\xi_x)^{n+1}_\xi$, respectively, which come from the source term of Eq. (8). Now a relative error, E, in the solution may be written as a function of only the geometric mapping parameters,

$$E=\frac{u^{n+1}-u}{u}=-\frac{1}{2}[(1+c\Delta\tau\bar{Q}-\nu\nabla\xi_x)(\nu\Delta\xi_x-c\Delta\tau Q)$$
$$+(\nu\nabla\xi_x-c\Delta\tau\bar{Q})-\nu\xi_{x_{j-1}}(\nu\nabla\Delta\xi_x-c\Delta\tau\nabla Q)] \tag{9}$$

Thus the relative error in executing one integration step is entirely dependent upon the geometric mapping for a given ν and number of mesh points. It is reasonable to assume that for some mappings this error is insignificant while for others it may be overwhelming. Indeed this is the case. Assume the specific mapping function given by

$$\xi(x)=\frac{e^{\beta x}-1}{e^\beta-1}\qquad \begin{matrix}0\le x\le 1\\ 0\le\xi\le 1\end{matrix} \tag{10}$$

where β is a parameter which controls the amount of coordinate stretching and $\beta=0$ is the limiting case, $\xi=x$. This mapping will be referred to as mapping I. Figure 1a illustrates the character of this mapping for various values of β. If the relative error is computed for this mapping with Eq. (9), the

result is that $E \equiv 0$ for any ν and any mesh spacing. Thus, no error is introduced into the solution due to this mapping. However, suppose the mapping function is given by

$$x(\xi) = \frac{e^{\beta\xi} - 1}{e^{\beta} - 1} \qquad \begin{matrix} 0 \le x \le 1 \\ 0 \le \xi \le 1 \end{matrix} \tag{11}$$

or

$$\xi(x) = \frac{1}{\beta} \ell n [1 - (1 - e^{\beta}) x]$$

This mapping will be called mapping II. Figure 1b illustrates the character of this mapping for various values of β. It can be shown that the relative error function in this case may be expressed as

$$E_j = \frac{-\nu K}{2} e^{(j-2)\theta} \{ (e^{2\theta} - 2\theta e^{\theta} - 1) + \nu K e^{(j-2)\theta} [(\theta - 1) e^{3\theta} + (1 - \theta^2) e^{2\theta} + e^{\theta} - (1 + \theta)] \} \tag{12}$$

where (note the symbol $\triangleq$ is used to indicate a definition)

$$\theta \triangleq -\beta \Delta\xi, \quad K \triangleq \frac{e^{\beta} - 1}{\beta}, \quad \Delta\xi = \frac{1}{J - 1}$$

and J is the number of mesh points. The subscript j indicates that the relative error is a function of position in the mesh for this mapping. Figures 2a and 2b illustrate the magnitude of this error for various values of β. These figures vividly demonstrate that large errors can result in just one step from the use of this mapping. A beta of 10 on these figures has a special significance in that it corresponds to the value required to obtain

$$(y_2 - y_1) / (y_J - Y_1) \simeq .0001$$

for the case when $J = 11$. This high degree of grid refinement is often required near a wall for high Reynolds number turbulent flow calculations, although for such calculations more than 11 points are required. It is important to point out that formally $E_j \simeq 0(\Delta\tau^3)$, which means two things. First, since MacCormack's scheme is second-order accurate in both time and space, i.e.,

$$u^{n+1} = u^n + \frac{\Delta\tau}{2} \left[\left(\frac{\partial u}{\partial \tau} \right)^n + \left(\frac{\partial u}{\partial \tau} \right)^{\overline{n+1}} \right] + 0(\Delta\tau^3)$$

then clearly the relative error formally reflects the accuracy of the integration scheme used. Second, in view of the gross errors possible with this mapping, it becomes necessary to question the very meaning of the formal order of accuracy of a method or scheme in this context. It is possible that the Taylor series representation of E_j in Eq. (12) is divergent for at least some values of β and $\Delta\xi$. This may explain the existence of extremely large errors which are formally claimed to be $0(\Delta\tau^3)$.

This example clearly shows the merit of a scheme which guarantees $u_j^{n+1} = u_j^n$ whenever $u_j^n = \text{const}$ for all j. For such a scheme, $E \equiv 0$ for all j and for all mappings. The fact that $E \equiv 0$ in the case of mapping I given by Eq. (10) is due to the linear dependence of the metric ξ_x on the transformed coordinate, ξ. That is, differentiating Eq. (10),

$$\frac{\partial \xi}{\partial x} = \frac{\beta}{e^{\beta} - 1} e^{\beta x} = \beta\xi + \frac{\beta}{e^{\beta} - 1}$$

so that Q and $\bar{Q}$ in Eq. (9) are given by $Q = \bar{Q} = (\xi_x)_\xi = \beta$ which has no spatial variation. Thus, $\Delta\xi_x / \Delta\xi \equiv (\xi_x)_\xi$, etc., and the terms in brackets in Eq. (9) all vanish. In contrast to

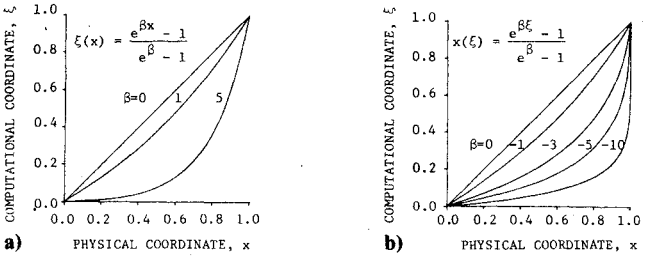

Fig. 1 Relation between physical and computational coordinates for a) mapping I and b) mapping II.

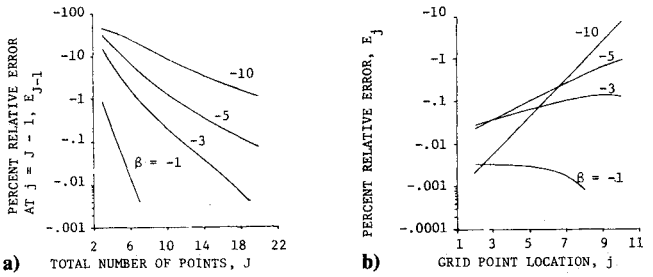

Fig. 2 Geometrically induced relative error with mapping II. a) at $j = J - 1$; b) distribution for $J = 11$.

this special case, the mapping of Eq. (11) yields a metric variation in terms of the transformed coordinate of

$$\frac{\partial \xi}{\partial x} = \frac{e^{\beta} - 1}{\beta e^{\beta\xi}}$$

which is highly nonlinear with $(\xi_x)_\xi = (1 - e^{\beta}) / e^{\beta\xi}$. Thus, for example, $\Delta\xi_x / \Delta\xi$ is not a very good approximation to $(\xi_x)_\xi$ and this is the source of the large relative error since the terms in brackets in Eq. (9) do not vanish for this case.

Before proceeding, a few words are needed with regard to multidimensional equations and nonlinear equations. The relative error for a multidimensional linear scalar equation in WCLF may be derived in the same manner as the expression for the one-dimensional example just presented. The resulting expression is more complicated and to conserve space will not be given here. As was the case in the one-dimensional problem, the relative error is dependent only upon the geometric mapping parameters once the value of ν and number of grid points are chosen. For the nonlinear problem, however, it is reasonable to expect, since the relative error will depend upon the solution itself, that some solutions will amplify the already present geometrically induced error while other solutions might tend to damp this error. In other words, the relative error induced by improper numerical treatment of the geometric mapping is problem dependent for nonlinear equations. Thus it is important that a numerical integration algorithm somehow eliminate this error source so as to enhance the reliability of the resulting algorithm. This is accomplished for the WCLF and SCLF of the equations as follows.

WCLF

The application of MacCormack's scheme to the WCLF of the transformed equations [Eq. (4)] yields:

Predictor

$$\overline{u^{n+1}} = u - \frac{\Delta\tau}{\Delta\xi} \Delta_i (\xi_t u + \xi_x f + \xi_y g) - \frac{\Delta\tau}{\Delta\eta} \Delta_j (\eta_t u + \eta_x f + \eta_y g) + \Delta\tau [(\xi_t)_\xi + (\eta_t)_\eta] u + \Delta\tau [(\xi_x)_\xi + (\eta_x)_\eta] f + \Delta\tau [(\xi_y)_\xi + (\eta_y)_\eta] g$$

Corrector

$$u^{n+1}=\frac{1}{2}\Big\{u+\overline{u^{n+1}}-\frac{\Delta\tau}{\Delta\xi}\nabla_i(\xi_t u+\xi_x f+\xi_y g)^{\overline{n+1}}$$

$$-\frac{\Delta\tau}{\Delta\eta}\nabla_j(\eta_t u+\eta_x f+\eta_y g)^{\overline{n+1}}+\Delta\tau[(\xi_t)_\xi+(\eta_t)_\eta]^{\overline{n+1}}\overline{u^{n+1}}$$

$$+\Delta\tau[(\xi_x)_\xi+(\eta_x)_\eta]^{\overline{n+1}}\overline{f^{n+1}}+\Delta\tau[\xi_y)_\xi+(\eta_y)_\eta]^{\overline{n+1}}\overline{g^{n+1}}\Big\}$$

The use of the product expansion formula $\Delta_i(AB)=A_{i+1}\Delta B+(\Delta A)B$ on the predictor equation yields

$$\overline{u^{n+1}}=u-\frac{\Delta\tau}{\Delta\xi}[\Delta_i(\xi_t)u+\Delta_i(\xi_x)f+\Delta_i(\xi_y)g]$$

$$-\frac{\Delta\tau}{\Delta\xi}\{(\xi_t)_{i+1}\Delta_i u+(\xi_x)_{i+1}\Delta_i f+(\xi_y)_{i+1}\Delta_i g\}$$

$$-\frac{\Delta\tau}{\Delta\eta}[\Delta_j(\eta_t)u+\Delta_j(\eta_x)f+\Delta_j(\eta_y)g]$$

$$-\frac{\Delta\tau}{\Delta\eta}\{(\eta_t)_{j+1}\Delta_j u+(\eta_x)_{j+1}\Delta_j f+(\eta_y)_{j+1}\Delta_j g\}$$

$$+\Delta\tau[(\xi_t)_\xi u+(\eta_t)_\eta u+(\xi_x)_\xi f+(\eta_x)_\eta f$$

$$+(\xi_y)_\xi g+(\eta_y)_\eta g]$$

Now suppose $u^n_{i,j}=\text{const}$ for all i,j. Then the terms in braces vanish since $\Delta_i u=u^n_{i+1}-u^n_i=0$, etc. Collection of terms in brackets results in the equation

$$\overline{u^{n+1}}=u-\Delta\tau\left[\frac{\Delta_i(\xi_t)}{\Delta\xi}-(\xi_t)_\xi\right]u-\Delta\tau\left[\frac{\Delta_j(\eta_t)}{\Delta\eta}-(\eta_t)_\eta\right]u$$

$$-\Delta\tau\left[\frac{\Delta_i(\xi_x)}{\Delta\xi}-(\xi_x)_\xi\right]f-\Delta\tau\left[\frac{\Delta_j(\eta_x)}{\Delta\eta}-(\eta_x)_\eta\right]f$$

$$-\Delta\tau\left[\frac{\Delta_i(\xi_y)}{\Delta\xi}-(\xi_y)_\xi\right]g-\Delta\tau\left[\frac{\Delta_j(\eta_y)}{\Delta\eta}-(\eta_y)_\eta\right]g$$

from which $\overline{u^{n+1}}=u$ at all points, provided all bracketed quantities vanish. This is possible if the metric derivatives in the source term [i.e., $(\xi_t)_\xi$, etc.] are computed numerically with the same difference operator that was used to evaluate the associated flux derivative. In this case

$$(\xi_t)_\xi\simeq\frac{\Delta_i(\xi_t)}{\Delta\xi},\qquad(\xi_x)_\xi\simeq\frac{\Delta_i(\xi_x)}{\Delta\xi}$$

and so on. Now that $\overline{u^{n+1}}=u^n$ at all points, the same procedure may be used on the corrector to yield $u^{n+1}=u^n$ provided

$$(\xi_t)^{\overline{n+1}}_{\xi}=\frac{\nabla_i(\xi_t^{\overline{n+1}})}{\Delta\xi}\qquad(\xi_x)^{\overline{n+1}}_{\xi}=\frac{\nabla_i(\xi_x^{\overline{n+1}})}{\Delta\xi}$$

and so on. The resulting predictor-corrector scheme may be written as:

Predictor

$$\overline{u^{n+1}}=u-\frac{\Delta\tau}{\Delta\xi}[(\xi_t)_{i+1}\Delta_i u+(\xi_x)_{i+1}\Delta_i f+(\xi_y)_{i+1}\Delta_i g]$$

$$-\frac{\Delta\tau}{\Delta\eta}[(\eta_t)_{j+1}\Delta_j u+(\eta_x)_{j+1}\Delta_j f+(\eta_y)_{j+1}\Delta_j g]$$

Corrector

$$u^{n+1}=\frac{1}{2}\Big\{u+\overline{u^{n+1}}-\frac{\Delta\tau}{\Delta\xi}[(\xi_t)_{i-1}\nabla_i u+(\xi_x)_{i-1}\nabla_i f$$

$$+(\xi_y)_{i-1}\nabla_i g]^{\overline{n+1}}-\frac{\Delta\tau}{\Delta\eta}[(\eta_t)_{j-1}\nabla_j u+(\eta_x)_{j-1}\nabla_j f$$

$$+(\eta_y)_{j-1}\nabla_j g]^{\overline{n+1}}\Big\}\qquad(13)$$

Note that no constraint has been placed on how the metrics ξ_t, ξ_x, ξ_y, η_t, η_x, and η_y are to be evaluated but only how their derivatives must be evaluated. This is not the case when the SCLF of the equations is used as is now shown.

SCLF

Application of MacCormack's scheme to the SCLF given by Eq. (5) yields:

Predictor

$$\overline{\left(\frac{u}{J}\right)^{n+1}}=\left(\frac{u}{J}\right)-\frac{\Delta\tau}{\Delta\xi}\Delta_i\left[\frac{\xi_t}{J}u+\frac{\xi_x}{J}f+\frac{\xi_y}{J}g\right]$$

$$-\frac{\Delta\tau}{\Delta\eta}\Delta_j\left[\frac{\eta_t}{J}u+\frac{\eta_x}{J}f+\frac{\eta_y}{J}g\right]$$

Corrector

$$\left(\frac{u}{J}\right)^{n+1}=\frac{1}{2}\left\{\left(\frac{u}{J}\right)+\overline{\left(\frac{u}{J}\right)^{n+1}}-\frac{\Delta\tau}{\Delta\xi}\nabla_i\left[\frac{\xi_t}{J}u+\frac{\xi_x}{J}f\right.\right.$$

$$\left.\left.+\frac{\xi_y}{J}g\right]^{\overline{n+1}}-\frac{\Delta\tau}{\Delta\eta}\nabla_j\left[\frac{\eta_t}{J}u+\frac{\eta_x}{J}f+\frac{\eta_y}{J}g\right]^{\overline{n+1}}\right\}$$

Expansion of the predictor equation using the product expansion formula previously introduced and recognition that

$$\Delta_i u=\Delta_i f=\Delta_i g=\Delta_j u=\Delta_j f=\Delta_j g=0$$

since $u_{i,j}=\text{const}$ for all i,j yields the equation

$$\left(\frac{u}{J}\right)^{n+1}=\left(\frac{u}{J}\right)-\Delta\tau\left\{\left[\frac{\Delta_i(\xi_t/J)}{\Delta\xi}+\frac{\Delta_j(\eta_t/J)}{\Delta\eta}\right]u\right.$$

$$\left.+\left[\frac{\Delta_i(\xi_x/J)}{\Delta\xi}+\frac{\Delta_j(\eta_x/J)}{\Delta\eta}\right]f+\left[\frac{\Delta_i(\xi_y/J)}{\Delta\xi}+\frac{\Delta_j(\eta_y/J)}{\Delta\eta}\right]g\right\}$$

Since the conditions are sought which cause $\overline{u^{n+1}}=u^n$ for all i,j it is natural to require the bracketed coefficients of f and g to vanish and the coefficient of u on the right-hand side to equal the coefficient of u on the left-hand side. This results in the conditions

$$\frac{\Delta_i(\xi_x/J)}{\Delta\xi}+\frac{\Delta_j(\eta_x/J)}{\Delta\eta}=0\qquad(14)$$

$$\frac{\Delta_i(\xi_y/J)}{\Delta\xi}+\frac{\Delta_j(\eta_y/J)}{\Delta\eta}=0\qquad(15)$$

$$\left(\frac{1}{J}\right)^{n+1}=\left(\frac{1}{J}\right)-\frac{\Delta\tau}{\Delta\xi}\Delta_i\left(\frac{\xi_t}{J}\right)-\frac{\Delta\tau}{\Delta\eta}\Delta_j\left(\frac{\eta_t}{J}\right)\qquad(16)$$

Equations (14) and (15) are rewritten with the use of the identities in Eq. (7) to yield

$$\frac{\Delta_i(y_\eta)}{\Delta\xi}+\frac{\Delta_j(-y_\xi)}{\Delta\eta}=0\qquad\frac{\Delta_i(-x_\eta)}{\Delta\xi}+\frac{\Delta_j(x_\xi)}{\Delta\eta}=0$$

These conditions are identically satisfied if x_ξ, x_η, y_ξ, y_η are approximated by forward differences such that

$$y_\eta \cong \frac{\Delta_j(y)}{\Delta\eta}, \quad x_\eta \cong \frac{\Delta_j(x)}{\Delta\eta}, \quad y_\xi \cong \frac{\Delta_i(y)}{\Delta\xi}, \quad x_\xi \cong \frac{\Delta_i(x)}{\Delta\xi} \tag{17}$$

In addition, Eq. (16) represents the condition resulting for a time-varying grid. This equation represents MacCormack's predictor applied to the identity

$$\left(\frac{1}{J}\right)_\tau + \left(\frac{\xi_t}{J}\right)_\xi + \left(\frac{\eta_t}{J}\right)_\eta = 0$$

which is called the geometric conservation law (GCL) by Thomas and Lombard[5] who first recognized the need for numerically solving this identity with the same integration scheme used for the SCLF of the transformed equations. The same process may be applied to the corrector equation to yield the following conditions,

$$\frac{\nabla_i(\xi_x/J)^{\overline{n+1}}}{\Delta\xi} + \frac{\nabla_j(\eta_x/J)^{\overline{n+1}}}{\Delta\eta} = 0$$

$$\frac{\nabla_i(\xi_y/J)^{\overline{n+1}}}{\Delta\xi} + \frac{\nabla_j(\eta_y/J)^{\overline{n+1}}}{\Delta\eta} = 0$$

$$\left(\frac{1}{J}\right)^{n+1} = \frac{1}{2}\left\{\left(\frac{1}{J}\right)^n + \left(\frac{1}{J}\right)^{\overline{n+1}} - \frac{\Delta\tau}{\Delta\xi}\nabla_i\left(\frac{\xi_t}{J}\right)^{\overline{n+1}} - \frac{\Delta\tau}{\Delta\eta}\nabla_j\left(\frac{\eta_t}{J}\right)^{\overline{n+1}}\right\}$$

where it follows that

$$y_\eta^{\overline{n+1}} \simeq \frac{\nabla_j(y)^{\overline{n+1}}}{\Delta\eta}, \quad x_\eta^{\overline{n+1}} \simeq \frac{\nabla_j(x)^{\overline{n+1}}}{\Delta\eta}$$

$$y_\xi^{\overline{n+1}} \simeq \frac{\nabla_i(y)^{\overline{n+1}}}{\Delta\xi}, \quad x_\xi^{\overline{n+1}} \simeq \frac{\nabla_i(x)^{\overline{n+1}}}{\Delta\xi} \tag{18}$$

The result is that $u^{n+1} = u^n$ for all i,j when $u^n = \text{const}$ for all i,j. The resulting predictor-corrector scheme may be written as:

Predictor

$$u^{\overline{n+1}} = u - \frac{\Delta\tau}{\Delta\xi}\left[(\xi_t)_{i+1}\Delta_i u + (\xi_x)_{i+1}\Delta_i f + (\xi_y)_{i+1}\Delta_i g\right]\frac{J^{\overline{n+1}}}{J_{i+1}} - \frac{\Delta\tau}{\Delta\eta}\left[(\eta_t)_{j+1}\Delta_j u + (\eta_x)_{j+1}\Delta_j f + (\eta_y)_{j+1}\Delta_j g\right]\frac{J^{\overline{n+1}}}{J_{j+1}}$$

Corrector

$$u^{n+1} = \frac{1}{2}\left\{\left(\frac{J^{n+1}}{J^n}\right)u^n + \left(2 - \frac{J^{n+1}}{J^n}\right)u^{\overline{n+1}} - \frac{\Delta\tau}{\Delta\xi}\left[(\xi_t)_{i-1}\nabla_i u + (\xi_x)_{i-1}\nabla_i f + (\xi_y)_{i-1}\nabla_i g\right]^{\overline{n+1}}\frac{J^{n+1}}{J_{i-1}^{\overline{n+1}}} - \frac{\Delta\tau}{\Delta\eta}\left[(\eta_t)_{j-1}\nabla_j u + (\eta_x)_{j-1}\nabla_j f + (\eta_y)_{j-1}\nabla_j g\right]^{\overline{n+1}}\frac{J^{n+1}}{J_{j-1}^{\overline{n+1}}}\right\} \tag{19}$$

where the metrics must be numerically computed from Eqs. (17) and (18) with the use of the identities in Eqs. (7).

Equations (13) for the WCLF and Eqs. (19) for the SCLF do not normally appear as they are written here. The present form is used, however, to provide an interesting comparison.

The major results to this point are now summarized. A reliable algorithm must be able to exactly reproduce a constant flowfield for all time. This requirement results in special treatment of some or all of the geometric mapping parameters for the WCLF and SCLF. Failure to satisfy this requirement can cause gross errors in the computed solution. This amounts to computing derivatives of metrics with finite differences for the WCLF with no requirements on the metrics themselves, while for the SCLF the metrics are computed with finite differences and the GCL equation must be solved numerically for problems with time-varying grids. The actual finite differences used for these geometric terms depend upon which numerical integration scheme is chosen to integrate the governing equations.

The fact that special conditions result for the WCLF and SCLF in order that exact reproduction of constant flowfield is possible suggests that some other form of the governing equations may be more desirable. Consider MacCormack's scheme applied to the NCLF of the equations [Eq. (6)]:

Predictor

$$u^{*\overline{n+1}} = u^* - \frac{\Delta\tau}{\Delta\xi}(\xi_t I + \xi_x A + \xi_y B)_{i+\alpha}\Delta_i u^* - \frac{\Delta\tau}{\Delta\eta}(\eta_t I + \eta_x A + \eta_y B)_{j+\alpha}\Delta_j u^*$$

Corrector

$$u^{*\overline{n+1}} = \frac{1}{2}\left\{u^* + u^{*\overline{n+1}} - \frac{\Delta\tau}{\Delta\xi}(\xi_t I + \xi_x A + \xi_y B)_{i-\alpha}^{\overline{n+1}}\nabla_i u^{*\overline{n+1}} - \frac{\Delta\tau}{\Delta\eta}(\eta_t I + \eta_x A + \eta_y B)_{j-\alpha}^{\overline{n+1}}\nabla_j u^{*\overline{n+1}}\right\} \tag{20}$$

where $0 \le \alpha \le 1$. Now if the solution at n is $u_{i,j}^{*n} = \text{const}$ for all i,j, then it is easy to see that application of Eqs. (20) for one step yields directly $u^{*n+1} = u^{*n}$. That is, the mapping parameters are uncoupled from the finite differences used in the integration scheme so that satisfaction of special conditions on the geometric parameters is not required for the NCLF in order to reproduce a constant flowfield exactly. This exact reproduction is satisfied automatically by the form of the equations. Unfortunately, the NCLF of the equations is not able to capture weak solutions correctly. This is what motivates the analyst to use a conservation law form. Consider now the result of applying MacCormack's scheme to the CRCLF of the equations given by Eq. (3):

Predictor

$$u^{\overline{n+1}} = u - \frac{\Delta\tau}{\Delta\xi}\left[(\xi_t)_{i+\alpha}\Delta_i u + (\xi_x)_{i+\alpha}\Delta_i f + (\xi_y)_{i+\alpha}\nabla_i g\right] - \frac{\Delta\tau}{\Delta\eta}\left[(\eta_t)_{j+\alpha}\Delta_j u + (\eta_x)_{j+\alpha}\Delta_j f + (\eta_y)_{j+\alpha}\Delta_j g\right]$$

Corrector

$$u^{n+1} = \frac{1}{2}\left\{u + u^{\overline{n+1}} - \frac{\Delta\tau}{\Delta\xi}\left[(\xi_t)_{i-\alpha}\nabla_i u + (\xi_x)_{i-\alpha}\nabla_i f + (\xi_y)_{i-\alpha}\nabla_i g\right]^{\overline{n+1}} - \frac{\Delta\tau}{\Delta\eta}\left[(\eta_t)_{j-\alpha}\nabla_j u + (\eta_x)_{j-\alpha}\nabla_j f + (\eta_y)_{j-\alpha}\nabla_j g\right]^{\overline{n+1}}\right\} \tag{21}$$

Again, $0 \le \alpha \le 1$ and $u^n_{i,j} = \text{const}$ for all i,j, then it is obvious by inspection of Eqs. (21) that $u^{n+1} = u^n$ for all i,j without imposing any special conditions on the metrics or their derivatives. Thus, the exact reproduction in this case is also automatically satisfied by the form of the equations. In addition, it is easy to see that Eqs. (21) are capable of capturing weak solutions since these equations with $\alpha = 1$ are identical to those derived for the WCLF [see Eqs. (13)] where special differencing was required on the metric derivatives in the source term (this follows provided one believes in the capturing capability of the WCLF). It is not the intention of the author to advocate the use of $\alpha = 1$ but rather to point out that such an α yields a scheme identical to the consistently formulated WCLF scheme.

The CRCLF requires no special consideration on how to compute the metrics or their derivatives and it has the ability to capture weak solutions. In addition, it requires fewer arithmetic operations to perform the calculation of the same representative quantity as shown in Table 1.

This table illustrates that when chaining† is used the actual number of operations are fewer for the SCLF but a divide is needed which requires far more computational effort than the additional two adds shown for the CRCLF. When the SCLF is used it may be more efficient to store the inverse of the Jacobian. Then the divide shown would instead be one extra multiply. This multiply would still require more computer time than the two adds for the CRCLF. In addition, if J^{-1} is stored, then in order to obtain u^{n+1} from $(uJ^{-1})^{n+1}$ a divide must still be performed at this point. If the grid is time invariant, then efficiency is gained if both J and J^{-1} are stored so that these divides are eliminated completely. Note, however, that for time-varying grids a great deal of additional effort will be required to solve the GCL equation along with the SCLF.

The next section contains simple numerical results which demonstrate the relative merits of the WCLF, CRCLF, and SCLF of the equations.

Numerical Results

The results in this section are categorized into three main groups. The first group deals with the shock-capturing ability of the CRCLF, WCLF, and SCLF. The second group is devoted to geometrically induced steady-state errors made with a model equation using the WCLF with inconsistent metric derivatives which prohibit satisfaction of the uniform flow reproduction test. The third group contains results of a study of the consequences of not satisfying the GCL equation when the SCLF is used on a space-marching problem.

Shock Capturing

Normally when the shock-capturing ability of a scheme or method is to be tested, a simple model problem is chosen such as the inviscid Burgers' equation in one dimension

$$u_t + \left(\frac{u^2}{2}\right)_x = 0 \qquad 0 \le x \le 1, \qquad 0 \le t$$

with discontinuous initial conditions such as

$$u(x,0) = \begin{cases} 1 & 0 \le x < d \\ 0 & d < x \le 1 \end{cases} \qquad 0 < d < 1$$

Unfortunately, a one-dimensional problem with a time-invariant grid is of no value for the test needed here since the SCLF solution reduces identically to the CRCLF solution in this case. To see this, examine the SCLF and CRCLF of the equation

$$u_t + f_x = 0$$

transformed by the time-invariant mapping $\tau = t$, $\xi = \xi(x)$. The SCLF is given by

$$\left(\frac{u}{J}\right)_\tau + \left(\frac{\xi_x f}{J}\right)_\xi = 0$$

where $J = \xi_x$, and the CRCLF is

$$u_\tau + \xi_x f_\xi = 0 \tag{22}$$

Note that the SCLF may be simplified to

$$\left(\frac{u}{\xi_x}\right)_\tau + f_\xi = 0$$

Application of MacCormack's scheme to the SCLF yields:

Predictor

$$\left(\frac{u}{\xi_x}\right)^{\overline{n+1}} = \left(\frac{u}{\xi_x}\right) - \frac{\Delta\tau}{\Delta\xi}\Delta f$$

Corrector

$$\left(\frac{u}{\xi_x}\right)^{n+1} = \frac{1}{2}\left[\left(\frac{u}{\xi_x}\right)^{\overline{n+1}} + \left(\frac{u}{\xi_x}\right) - \frac{\Delta\tau}{\Delta\xi}\nabla f^{\overline{n+1}}\right]$$

The predictor may be rewritten as

$$u^{\overline{n+1}} = \frac{\xi_x^{\overline{n+1}}}{\xi_x} u - \xi_x^{\overline{n+1}} \frac{\Delta\tau}{\Delta\xi}\Delta f$$

but for a time-invariant grid, $\xi_x^{\overline{n+1}} = \xi_x$ so

$$u^{\overline{n+1}} = u - \frac{\Delta\tau}{\Delta\xi}\xi_x \Delta_f$$

Likewise the corrector can be simplified to

$$u^{n+1} = \frac{1}{2}\left(u^{\overline{n+1}} + u - \frac{\Delta\tau}{\Delta\xi}\xi_x \nabla f^{\overline{n+1}}\right)$$

Table 1 Typical operation count summary for the various equation forms

Operation count to compute the ξ-direction contribution from the terms $\xi_t u_\xi + \xi_x f_\xi + \xi_y g_\xi$ for a scalar equation with $\Delta\xi = 1$ and assuming u, f, g, ξ_t, ξ_x, ξ_y, and J are already computed using equivalent effort:

CRCLF $\xi_t u_\xi + \xi_x f_\xi + \xi_y g_\xi$

WCLF $(\xi_t u + \xi_x f + \xi_y g)_\xi - (\xi_t)_\xi u - (\xi_x)_\xi f - (\xi_y)_\xi g$

SCLF $\left(\dfrac{\xi_t u + \xi_x f + \xi_y g}{J}\right)_\xi$

n/m[a]	WCLF	SCLF[b]	CRCLF
Add-subtract	11/9[a]	5/3	5/5
Multiply	9/6	6/3	3/3
Divide	0/0	2/1	0/0

[a] n = without chaining, m = with chaining. [b] This does not include the fact that the GCL equation must be solved with the SCLF for a time-varying grid.

†Chaining refers to the reuse of already calculated quantities. For example, calculation of $\Delta_i(A_i) = A_{i+1} - A_i$ at $i=2$ requires evaluation of A_3 and A_2 while at $i=3$ evaluation of A_4 and A_3 is required, but A_3 was already determined for $i=2$ so it need not be recalculated.

This predictor-corrector scheme is exactly that which would result from applying MacCormack's scheme directly to the CRCLF [Eq. (22)] with the metric evaluated at point j. Thus the two forms of the transformed equations yield the same difference scheme and thus identical numerical results for a one-dimensional equation and time-invariant grid. Recall that the CRCLF was also shown to yield results identical to the consistently formulated WCLF when the metric was evaluated at $j+1$ for a forward-differenced flux term and $j-1$ for a backward-differenced flux term. This result is true even for multidimensional equations and time-varying grids.

The preceding comments were verified by numerical experiments on the model equation

$$u_t + \left(\frac{u^2}{2}\right)_x = 0 \qquad 0 \le x \le 1, \qquad 0 \le t$$

which was mapped by $\tau = t$, $\xi = \xi(x)$ with initial conditions

$$u_j^0 = \begin{cases} 10 & j = 1 \\ 2 & j = 2,3,\ldots,J \end{cases}$$

Figure 3 illustrates the numerical solutions to the CRCLF, WCLF, and SCLF for the case where mapping II was applied. This figure shows that the postshock oscillations are damped somewhat for the consistent WCLF or CRCLF with offset metrics. The exact solution is shown for comparison.

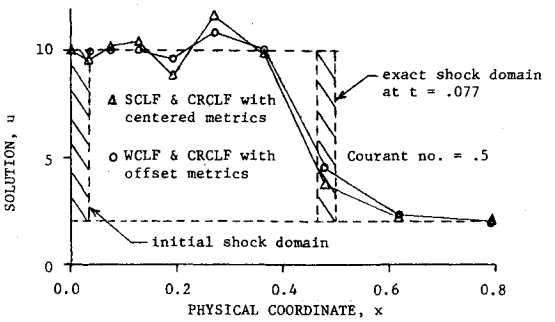

Fig. 3 Shock capturing and SCLF, CRCLF, WCLF equivalence for inviscid Burgers' equation with mapping II and $\beta = 2$.

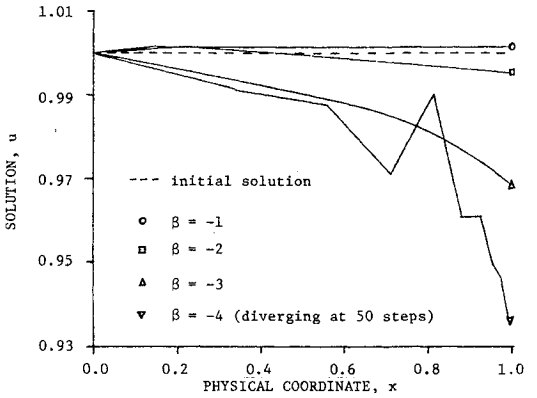

Fig. 4 Steady-state solution to one-dimensional wave equation in WCLF with mapping II and analytical metric derivative in source term.

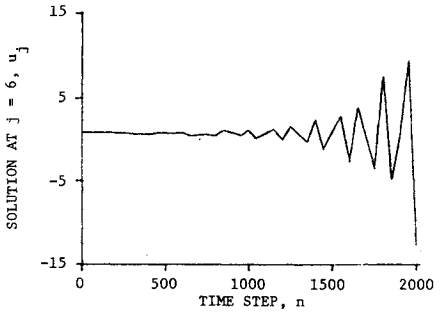

Fig. 5 Solution time history for one-dimensional wave equation in WCLF with mapping II, $\beta = -4$, and analytic metric derivative in source term.

Steady-State Errors of Inconsistent WCLF

A source term appears in the WCLF of the transformed equations of interest. This term contains derivatives of metrics. The uniform flow reproduction requirement imposes a restriction on how to evaluate these derivatives. An error results if this restriction is ignored. A simply study of the nature of this error is conducted by considering the one-dimensional first-order wave equation given in WCLF in transformed coordinates as

$$u_\tau + (c\xi_x u)_\xi - c(\xi_x)_\xi u = 0 \qquad 0 \le \xi \le 1, \quad 0 \le \tau$$

with initial condition $u(\xi,0) = 1$. The boundary conditions are $u(0,\tau) = 1$ and $u(1,\tau) = u(1 - c\Delta\tau, \tau - \Delta\tau)$. The exact steady-state solution to this problem is $u(\xi,\infty) = 1$. The numerical steady-state solution to this problem using MacCormack's scheme with 11 grid points is shown in Fig. 4 for mapping II at various values of β. Note that at $\beta = -3$ the steady-state error at $x = 1$ is 3%, while at $\beta = -4$ the solution is actually diverging. This divergence is seen clearly by examining the solution at a typical point as time progresses. This is shown in Fig. 5. It should be noted that $\beta = -4$ does not represent a severe coordinate stretching, yet a divergent solution results.

The primary purpose for using mappings is to place more grid points in regions where dependent variables are changing rapidly. This is especially true in viscous flow calculations where the grids must resolve the flow details in wall boundary layers. A mapping which is frequently used in viscous flow grids is due to Roberts[9] and is given by

$$\xi(x) = -1 - \ln\left(\frac{\beta + 1 - x}{\beta - 1 + x}\right) \Big/ \ln\left(\frac{\beta + 1}{\beta - 1}\right) \qquad 1 < \beta < \infty$$

where $\beta = \infty$ corresponds to the degenerate case $\xi = x$ and $\beta = 1$ implies infinite clustering at $\xi = 0$. This mapping will be called mapping III and is shown in Fig. 6 for various values of β. A study of the steady-state solution errors resulting from this mapping on an 11 point grid is summarized in Fig. 7. This figure reveals that for a moderate amount of stretching of $\beta = 1.005$, a 30% error results in the steady-state solution at $x = 1$. The solution divergence behavior present with $\beta = -4$ for mapping II did not appear for mapping III, even for $\beta = 1.0001$. However, a 30% steady-state error is intolerable.

The SCLF and GCL Equation

The SCLF of the transformed flow equations is widely used today for solving fluid flow problems. More often than not, however, the GCL equation is not correctly satisfied numerically. This may not present any difficulties for problems in which only the steady-state solution is of interest. However for problems with unsteady grids in time and space-marching problems, such as those for which the parabolized Navier-Stokes (PNS) equations are solved, the errors resulting from failure to numerically satisfy the GCL equation may be important. A study of this error is made by solving the Euler equations for supersonic flow over a two-dimensional body. The transformed equations in SCLF are given by

$$\left(\frac{f}{J}\right)_\xi + \left(\frac{\eta_x}{J} f + g\right)_\eta = 0$$

where the mapping $\xi = x$ and $\eta = \eta(x,y)$ has been applied and ξ is the marching direction. The GCL identity is

$$\left(\frac{1}{J}\right)_\xi + \left(\frac{\eta_x}{J}\right)_\eta = 0$$

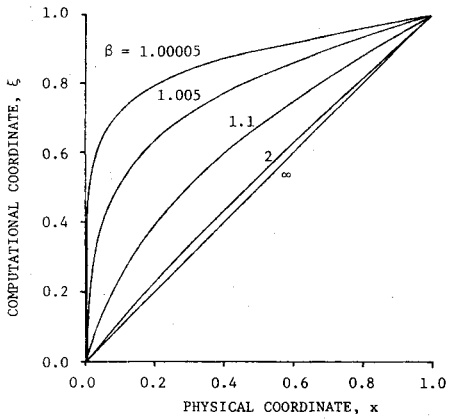

Fig. 6 Relation between physical and computational coordinates for mapping III.

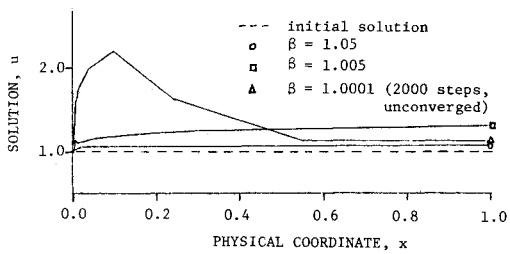

Fig. 7 Steady-state solution for one-dimensional wave equation in WCLF with mapping III and analytic metric derivative in source term.

The vectors f and g are the usual Cartesian flux vectors associated with the continuity and Euler momentum equations. The energy equation is simply: total enthalpy = const. The CRCLF of the transformed equations is given by

$$f_\xi + \eta_x f_\eta + \eta_y g_\eta = 0$$

The equations in SCLF and CRCLF are solved for two body shapes using MacCormack's standard unsplit predictor-corrector scheme. These two shapes represent a sharp-cornered expansion and a sharp-cornered compression as shown in Fig. 8. The freestream Mach number is 2 and the base wedge angle is 10 deg. Note that the GCL identity is not solved numerically for the SCLF. The outer shock is fitted explicitly so that the computational domain lies between this shock and the body. The calculations begin at $\xi = x = 1$ with the exact wedge solution. The grid of 10 points is distributed between the outer shock and the body according to mapping II with $\beta = 5$ (see Fig. 1b). The sharp corner in both the expansion and compression cases occurs at $\xi = x = 1.5$. The boundary condition used at the body is a simple wave correction procedure due to Abbett.[10] The metrics used in the SCLF and CRCLF are obtained analytically.

The results of marching down these two bodies with the SCLF and CRCLF codes are shown in Figs. 9 and 10. Figure 9 shows the pressure distribution in the physical coordinate y at an axial station just ahead of the expansion/compression corner. This figure clearly illustrates both a surface error of 2% and an anomaly at the shock for the SCLF code with a grid of 10 points. These errors are not present in the solution from the CRCLF. Also shown in Fig. 9 is the SCLF solution for a grid of 20 points. The errors are significantly reduced as expected, but are still present.

The steady-state error problem discussed for the model wave equation in the previous subsection shows up again in Figs. 10a and 10b. The body pressure distribution is presented for the expansion problem in Fig. 10a. This figure illustrates that the SCLF exhibits an error buildup of about 2% just ahead of the sharp expansion. This error continues to build

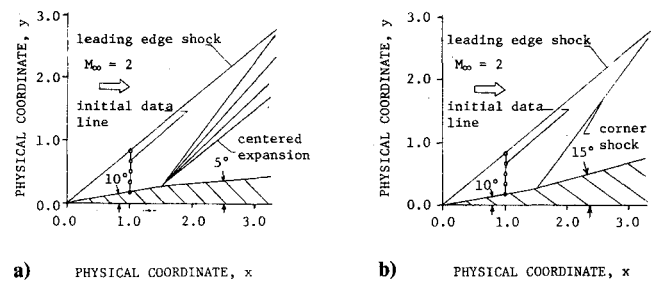

Fig. 8 Supersonic flow test geometries for a) sharp expansion and b) compression tests of SCLF and CRCLF.

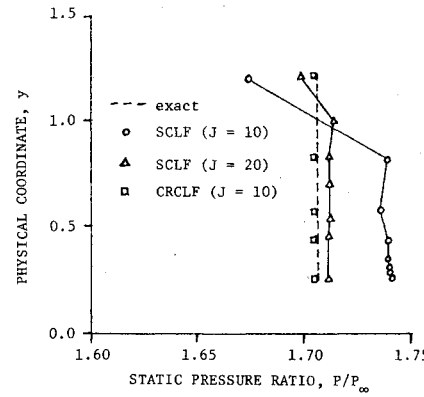

Fig. 9 Vertical static pressure distribution just ahead of expansion/compression corner at $\xi = x = 1.49$.

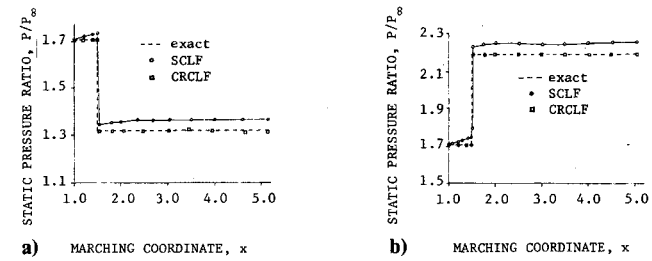

Fig. 10 Surface static pressure distribution: a) sharp expansion; b) sharp compression.

aft of the expansion to reach a steady-state error of about 3.8% at $\xi = x = 5$. This error is, of course, not present in the CRCLF solution. A very similar trend is observed for the compression problem in Fig. 10b, except that the steady-state error is lower at 2.8%.

Conclusions

A simple test for exact reproduction of uniform flow is exploited to yield conditions on the evaluation of the geometry derivative information for problems in which generalized mappings are used with the equations written in either WCLF or SCLF. No special conditions exist for the NCLF or CRCLF of the transformed equations. When the condition is satisfied for the WCLF, consistent finite-difference equations result which are shown to be exactly equivalent to those resulting from the CRCLF with the metric coefficients evaluated at $j-1$ for backward-differenced flux terms and $j+1$ for forward-differenced flux terms. Thus identical solutions are produced by the CRCLF with these offset metric evaluations and by the consistent WCLF. In addition to this equivalence, it is also shown that identical finite-difference schemes are produced by the CRCLF with the metric coefficients evaluated at point j and by the SCLF for one-dimensional problems with time-invariant grids. This equivalence builds confidence in the shock-capturing ability of the CRCLF.

Failure to satisfy the special condition for the WCLF is shown to lead to large steady-state errors for a model problem with mapping III and even divergence of the solution for mapping II with moderate stretching. Failure to satisfy the GCL condition for the SCLF is shown to give rise to significant errors on two simple inviscid supersonic flow problems when mapping II is used.

Both the consistently formulated WCLF and SCLF may be used. They require some analysis to determine the consistency conditions on the mapping parameters. This analysis must be done for each integration scheme used. The present work illustrates the analysis for MacCormack's scheme. For time-varying grids the SCLF requires the additional numerical solution of the GCL identity equation with the same integration scheme used for the transformed equations. Finally, both the WCLF and SCLF of the equations require more computational effort than the CRCLF. In addition, the CRCLF can capture shocks and yields qualitatively similar solutions to both the WCLF and SCLF.

More work is needed on the idea of geometrically induced errors, particularly for some of the currently popular implicit schemes and their use in space-marching applications such as parabolized Navier-Stokes equations.

References

[1] Viviand, H., "Conservative Forms of Gas Dynamic Equations," *La Recherche Aérospatiale,* No. 1, Jan.-Feb. 1974, pp. 65-68.

[2] Steger, J. L., "Implicit Finite-Difference Simulation of Flow About Arbitrary Geometrics with Application to Airfoils," AIAA Paper 77-665, June 1977.

[3] Hindman, R. G., "A Two-Dimensional Unsteady Euler-Equation Solver for Flows in Arbitrarily Shaped Regions Using a Modular Concept," Ph.D. Dissertation, Iowa State University, Ames, Iowa, 1980.

[4] Pulliam, T. H. and Steger, J. L., "Implicit Finite-Difference Simulations of Three-Dimensional Compressible Flow," *AIAA Journal,* Vol. 18, Feb. 1980, pp. 159-167.

[5] Thomas, P. D. and Lombard, C. K., "The Geometric Conservation Law—A Link Between Finite-Difference and Finite-Volume Methods of Flow Computation on Moving Grids," AIAA Paper 78-1208, July 1978.

[6] Lombard, C. K., Davy, W. C., and Green, M. J., "Forebody and Base Region Real-Gas Flow in Severe Planetary Entry by a Factored Implicit Numerical Method, Part I: Computational Fluid Dynamics," AIAA Paper 80-0065, Jan. 1980.

[7] Thomas, P. D., "Numerical Method for Predicting Flow Characteristics and Performance of Nonaxisymmetric Nozzles—Theory," NASA CR-3147, Sept. 1979.

[8] MacCormack, R. W., "The Effect of Viscosity in Hypervelocity Impact Cratering," AIAA Paper 69-354, April-May 1969.

[9] Roberts, G. O., "Computational Meshes for Boundary Layer Problems," *Lecture Notes in Physics,* Springer-Verlag, New York, 1971, pp. 171-177.

[10] Abbett, M. J., "Boundary Condition Computational Procedures for Inviscid Supersonic Steady Flow Field Calculations," Aerotherm Corp., Mountain View, Calif., Final Rept. 71-41, 1971.